APERIODIC WAVEFORMS WITH MISMATCHED FILTERING FOR TARGET DETECTION IN HEAVY CLUTTER. PART I - SIMO RADAR ARCHITECTURE

Y. I. Abramovich[†] *G. San Antonio*[‡] *G. J. Frazer*[^]

[†]WR Systems Ltd, Fairfax, VA, USA
[‡]Naval Research Laboratory, Washington DC, USA
[^]NSI Division, DSTO, Australia

ABSTRACT

Periodic waveforms used for most radar operations in heavy clutter often suffer from range-folding and/or Doppler frequency aliasing effects. Aperiodic waveforms with a "thumbtack" ambiguity function do not have range and/or Doppler ambiguities, but due to the relatively high sidelobe levels cannot support the high sub-clutter visibility required in many applications. In this paper, we demonstrate that for typical HF OTHR scenarios, aperiodic waveforms and mismatched filtering can provide the required level of sub-clutter visibility with acceptable SNR degradation. Theoretical results are complemented by experimental validation.

Index Terms— HF radar, OTHR, waveforms, mis-match filtering, aperiodic

1. INTRODUCTION

High frequency Over-the-Horizon Radar (HF-OTHR) and a number of other radar systems operate in the presence of very strong reflections from the Earth's surface. Moving target detection in such radars requires a very high level of sub-clutter visibility, i.e. a very high level of clutter sidelobe suppression at Doppler frequencies occupied by detected targets [1]. In practical applications, the level of these sidelobes (with respect to the ambiguity function main peak) should exceed 70dB for reliable target detection. The time-bandwidth product of the coherently processed radar waveform is limited by target motion and ionospheric dispersion, and for typical air-detection mode, it is does not exceed 40–50 dB, with bandwidth varying within 8–30kHz, and coherent integration time CIT 2–4s. Since this time-bandwidth product is >20dB below the required sub-clutter visibility, periodic waveforms such as pulse trains or periodic linear frequency modulated continuous waveforms (LFMCW) are typically used in such radars. With appropriate tapers both in the fast-time and slow-time domains, range and Doppler sidelobes are reduced to the required level. Range ambiguities in $\pm nT_r$, $n = 1, \ldots, N$ and Doppler frequency ambiguities in $\pm\frac{k}{T_r}$, $k = 1, \ldots, K$, with T_r being a repetition period, limit the "sidelobe-free" area around the main peak to its maximum level of four, established by Price and Hofstetter in 1965 [2].

Under favorable propagation conditions, with no multi-hop or homogeneous within-hop ionospheric propagation, this "tapered" Doppler filtering of periodic waveforms provides the required sub-clutter visibility and reliable target detection, while ambiguity in target range and/or Doppler frequency estimation is resolved by waveform jitter [3]. Specifically, applying two consecutive CITs with periodic waveforms with different repetition interval, in most practical cases, allows for this ambiguity to be resolved. Propagation conditions are not always favorable and with different ionospheric conditions over different "legs" of multi-hop propagation, the range folding effect "brings in" range folded spread (in Doppler frequency) clutter that may severely limit sub-clutter visibility. Methods that shift the ambiguity by "shearing" the "nails" within the "bed-of-nails" type ambiguity function, suggested for example in [4], have their limits. In particular they are ineffective if the total clutter spread (at different legs) exceeds the repetition frequency, and even when it works, it can support appropriate detection for either approaching or receding targets but not both concurrently. Therefore, for operating in difficult propagation conditions, such for example, as in the presence of range-folded Auroral clutter [5], periodic or quasi-periodic waveforms with a "bed-of-nails" ambiguity function, may not be appropriate.

It has been known for a considerable time that a properly designed mismatch filter can provide efficient mitigation of cross-ambiguity function sidelobes in a certain limited area of the range-Doppler frequency plane [6, 7, 8]. Strictly speaking, with M element mismatch filters, where $M \geq TB$, $TB = T_{\text{CIT}}B$, T_{CIT} is the coherent integration interval (waveform duration), B is the waveform bandwidth, up to N points on this plane may be driven to zero [9]. Yet, the white-noise SNR losses that depend on the type of waveform and configuration of the rejected area with respect to the cross-ambiguity function origin (target position), may be too significant. Therefore a study on the potential efficiency of mismatched filtering for relevant HF-OTHR scenarios is required. It is important to recall that practical application of

mismatched filtering has not been effective due to additional mismatch between the presumed (designed) waveform and the actual transmitted waveform. Digital waveform generation (DWG) and direct digital receiver (DDRx) technology, being broadly introduced into HF-OTHR radar design, alleviates this problem by accurately measuring the actual waveform for mismatch filter design. Nonetheless, experimental trials on the efficiency of practical mismatch filter implementation is still required for validation of the mismatch filtering methodology.

2. MISMATCHED FILTERING OF NOISE-LIKE WAVEFORMS FOR HF-OTHR APPLICATIONS

Let us consider the noise-like waveforms with their close to ideal "thumb-tack" ambiguity function and the mean sidelobe level equal to $-10\log N$ dB, where $TB = T_{\text{СП}}B$ is the time-bandwidth product. Let us consider typical air-mode LFMCW waveforms for comparison, introduced in [4].

Specifically, the bandwidth B=10kHz, waveform repetition frequency WRF=31.25Hz and the number of repetition periods P equal to P=128, which makes $T_{\text{СП}}$=4.096s with $TB = T_{\text{СП}}B$ = 40960.

According to [4] strong clutter returns from distances above 8000nm may be ignored, i.e. any returns beyond 1100 range resolution cells from a "zero" range, could be ignored. Moreover, in the introduced example in [4], all clutter returns are distributed within the ranges from 1110nm to 6570nm, which is only 5460nm or 10112km or 675 range cells.

Doppler spectra of these clutter returns are range-dependent with a strong range-dependent shift of its central frequency, as follows from plate 2 in [4]. Specifically this shift leads to the "spread clutter" effect when traditional periodic waveforms are used due to the range folding effect. Yet, at any range, the width of the Doppler spectra is reasonably narrow <4Hz, centered at the changing with range center frequency. Specifically this range-dependent property of the quite narrowband clutter Doppler spectrum, made efficient the proposed in [4] technique with slow-time (from sweep to sweep) LFMCW. The total area in the range-Doppler frequency plane occupied by these clutter returns is equal to 675 x 16 = 10800 for the waveform with time-frequency bandwidth N=40960.

Therefore, if ultimately for each resolution cell with a potential target present a specifically tailored optimum mismatch filter has to be designed, this filter has to suppress cross-ambiguity function sidelobes over the area that does not exceed $A_c = 0.26N$. Naturally, if a larger area A_s may be rejected by a single mismatched filter, with acceptable SNR degradation, then this single mismatched filter may be used for target detection within the "cleared" area $(A_s - A_c)$. This example demonstrates the range of practically relevant parameters that need to be explored.

For noise-like waveforms with close to ideal "thumb-tack" ambiguity functions, efficiency of the mismatch filtering depends mainly on the dimension of the suppressed area. For this reason, we investigate the efficiency of mismatch filters with a rectangular suppressed area:

$$A_c = \begin{cases} -\frac{N_r}{2}\tau_0 \le \tau \le \frac{N_r}{2}\tau_0 \qquad \tau_0 = \frac{1}{B} \\ -\frac{N_d}{2T_{\text{СП}}} < f \le \frac{N_d}{2T_{\text{СП}}} \end{cases} \tag{1}$$

with the target position at $\tau_0 = 0$, $f = f_0$, and

$$\begin{aligned} f_0 &> \tfrac{N_d}{2T_{\text{СП}}} \\ f_0 &< -\tfrac{N_d}{2T_{\text{СП}}} \end{aligned} \tag{2}$$

where N_r, N_d is the number of range (Doppler) resolution cells correspondingly within the clutter zone A_c.

According to equation (1) and equation (2) the target resolution cell is placed in the center of the "clutter" range extent, but out of the Doppler frequency band occupied by clutter.

The optimum (one that maximizes the output signal-to-clutter plus ratio) mismatched filter is calculated as

$$W = \frac{R^{-1}S(i_{rng}, k_{dop})}{S^H(i_{rng}, k_{dop})R^{-1}S(i_{rng}, k_{dop})} \tag{3}$$

and

$$R = \sum_{i=-\frac{N_r}{2}}^{\frac{N_r}{2}} S(i,0)S^H(i,0) \odot D(N_d) + \sigma_n^2 I \tag{4}$$

where

$$D(N_d) = \left[\frac{\sin(\frac{\pi N_d}{N}(n-m))}{\frac{\pi N_d}{N}(n-m)}\right] \quad n, m = 1, \ldots, N \tag{5}$$

with $S(i_{rng}, k_{dop})$ the radar waveform shifted in range and Doppler frequency by $\frac{i}{B}$ and $\frac{k}{T_{\text{СП}}}$ resolution cells correspondingly. $\sigma_n^2 = S^H S\sigma_{\text{load}}^2$, is the diagonal loading factor acting for the white noise (normalized) power.

The efficiency of mismatched filtering is assessed by the median sidelobe level over rejection region relative to peak response (equal to one according to equation (3)), which we associate with sub-clutter visibility (SCV) and by the signal-to-white noise ratio (SWNR) loss factor:

$$\varrho = \frac{|W^H S|^2}{W^H W \cdot S^H S} \tag{6}$$

In the examples, introduced below, the target coordinates have been fixed ($i_{rng} = 0$ and $k_{dop} = -5$) as well as the width of the Doppler band $N_d = 4$, while $N = T_{\text{СП}}B$ and the range extent of the suppressed N_r zone is varied.

In Figure 1 we illustrate the cross-ambiguity function "map" for N=20000 and N_r=1000 which for N_d=4. With A_c=4000 and A_c/N=0.2 this example is sufficiently close to

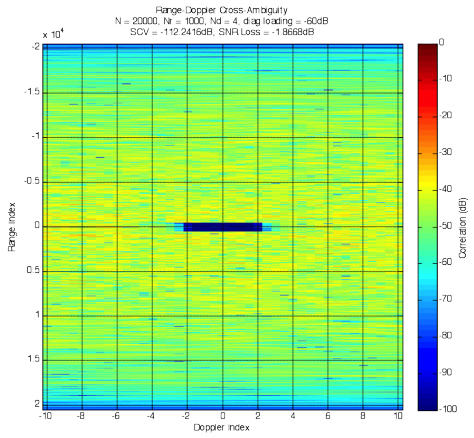

Fig. 1. N=20000 and N_r=1000 which for N_d=4. Range-Doppler cross-ambiguity function.

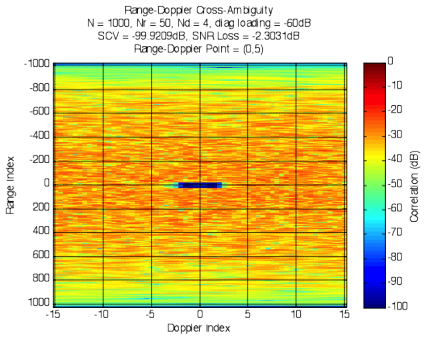

Fig. 2. N=1000 and N_r=50 which for N_d=4. Target position ($i_{rng} = 0$ and $k_{dop} = 5$). Range-Doppler cross-ambiguity function.

the considered practical example in [4]. For diagonal loading at the -60dB level, for this case, we get SCV= -112.24dB and ϱ_c= -1.87dB

It can be seen that the required high SCV is achieved with SWNR losses comparable with the SWNR losses associated with the standard "taper" approach used with conventional periodic waveform supporting similar SCV.

In Table 1 we introduce the results of similar calculations for noise-like waveforms with various time-bandwidth products $T_{\text{CIT}}B$ and various dimensions of the clutter zone A_c for the same target position ($i_{rng} = 0$ and $k_{dop} = 5$).

One can see that indeed the efficiency of mismatched filtering for "thumb-tack" ambiguity function sidelobe suppression depends on the A_c/N ratio, and satisfactory results can be obtained for A_c/N<0.2 More detailed insight into mismatched filter performance is provided by Figure 2 through Figure 5. In Figure 2 we introduce data for $TB = T_{\text{CIT}}B$=1000, N_r=50, N_d=4, A_c/N=0.2 and target coordinates (0,5) as per Table 1. Here, in Figure 2, in addition to the "colourmap" of the entire cross-ambiguity function as per Figure 1, we introduce the cross-sections through the range ($i_{rng} = 0$) in Figure 3 and Doppler frequency ($k_{dop} = 5$)

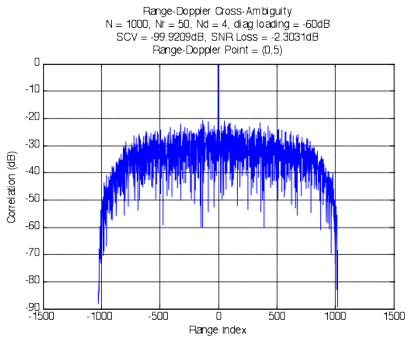

Fig. 3. N=1000 and N_r=50 which for N_d=4. Target position ($i_{rng} = 0$ and $k_{dop} = 5$). Range-slice of range-Doppler cross-ambiguity function.

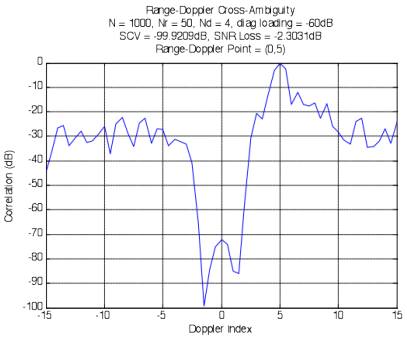

Fig. 4. N=1000 and N_r=50 which for N_d=4. Target position ($i_{rng} = 0$ and $k_{dop} = 5$). Doppler-slice of range-Doppler cross-ambiguity function.

in Figure 4 of the target. One can see that deep mitigation of the clutter area A_c did not impact the shape of the rest of the "thumb-tack" like ambiguity function, with the median sidelobe level ∼-28dB. Additionally, in Figure 5 we introduce here the amplitudes of the noise-like waveform and the mismatch filter response. One can recognize the familiar "tapering" at the beginning and end of the CIT introduced by this optimal filter. While most of the results are presented for a particular target positioned at ($i_{rng} = 0$ and $k_{dop} = 5$) in Figure 6 we introduce similar results calculated for a different target positioned at ($i_{rng} = 0$ and $k_{dop} = -10$). One can see that the mismatched filter performance practically does not depend on the target coordinate, as long as this coordinate is outside of the rejected "clutter zone". For noise-like waveforms with this "thumb-tack" like ambiguity function, this property is clearly anticipated.

3. EXPERIMENTAL VALIDATION OF MISMATCHED FILTER EFFICIENCY

The following experimental set-up has been used for validation. A digital arbitrary waveform generator (AWFG) is used to generate a random phase sequence at the rate 250kHz, producing 25000 samples. Then a digital FIR filter with 10kHz

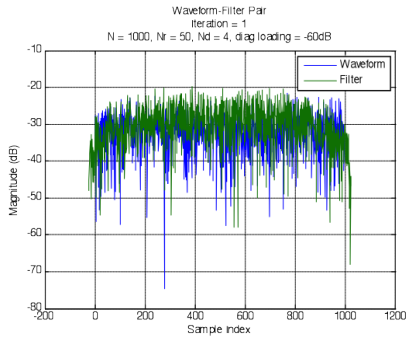

Fig. 5. N=1000 and N_r=50 which for N_d=4. Target position ($i_{rng} = 0$ and $k_{dop} = 5$). Waveform and filter magnitude.

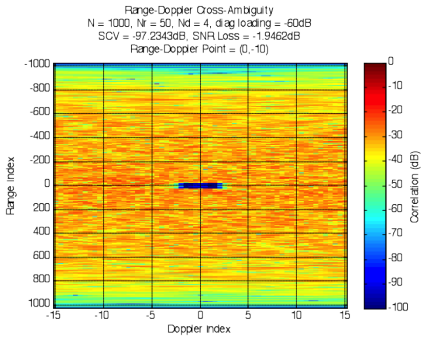

Fig. 6. N=1000 and N_r=50 which for N_d=4. Target position ($i_{rng} = 0$ and $k_{dop} = -10$). Range-Doppler cross-ambiguity function.

bandwidth has been used to limit the bandwidth and to convert the waveform into the noise-like waveform, with "random-like" amplitude and phase modulation. The output signal of the AWFG has been captured by a direct digital receiver (DDRx) at a sample rate of 125kHz, and decimated at its output to 25kHz, producing 2500 samples at 25kHz rate. The total duration of this waveform is therefore 0.1s with time-bandwidth product $T_{\text{CIT}}B$=1000 (as per the example in Table 1. Yet, mismatch filter design and its performance assessment has been conducted for over-sampled representation of this waveform by 2500 samples at 25kHz rate.

The "theoretical" or "programmed" waveform has been pre-calculated using an ideal transformation of the initial prescribed random phase sequence, and this "programmed" waveform differs from the one actually captured by the receiver.

In what follows we compare the results of mismatch filter efficiency for both "programmed" and the actually captured waveform, when this filter is designed for the ideal "programmed" waveform. The mismatch between the "programmed" and the actual waveforms causes some SCV degradation that is analyzed in this study. Results of this comparison are presented in Table 2.

First of all notice that 20dB less diagonal loading (-80dB instead of -60dB) transpired into 20dB higher SCV values for

Table 1. $N_d = 4$; $\sigma^2_{load} = -60$dB

N	N_r	A_c/N	SCV (dB)	ϱ_l dB
1e3	50	0.2	-98.5	-2.14
1e3	100	0.4	-89.8	-5.67
5e3	50	0.04	-108.7	-0.52
5e3	100	0.08	-108.7	-0.84
5e3	200	0.16	-107.97	-1.45
5e3	500	0.4	-97.4	-5.3
10e3	200	0.08	-111.3	-0.83
10e3	500	0.2	-109.0	-1.9
10e3	1000	0.4	-98.98	-5.5
20e3	1000	0.2	-112.2	-1.87
20e3	2000	0.4	-103.16	-5.47

Table 2. N=2500, B=10kHz, T_{CIT}=0.1s, f_D=25kHz, $N_d = 4$; $\sigma^2_{\text{load}} = -80$dB. Ratios are in dB.

N_r	A_c/N	SCV$_{id}$	SCV$_{ac}$	ϱ_{id}	ϱ_{ac}
50	0.08	-121.3	-84.7	-1.95	-1.95
100	0.16	-121.2	-85.2	-2.59	-2.59
150	0.24	-118.6	-84.7	-3.58	-3.58
200	0.32	-115.1	-83.45	-4.938	-4.940

the "theoretical" ideal waveform, but also increased SWNR losses by >1dB. Unfortunately, due to the mismatch between the ideal and the actually captured waveform, the actual SCV is limited to 84–85dB, while the SWNR losses remain practically the same.

Apart from SCV limitations imposed by mismatch, this example demonstrates that diagonal loading should be selected to make the "theoretical" (ideal) SCV comparable with the actually realizable value in order to minimize the associated SWNR losses. Note that for the waveform with time-bandwidth product of 1000 only, SCV limitations by 85dB due to waveform inaccuracies is a very satisfactory value since for practical waveforms with this product equal to 40000 we may expect ∼16dB improvement. Finally, note that if the mismatched filter is designed for the actually captured transmitted waveform, none of the losses discussed would occur.

4. CONCLUSIONS

The introduced analysis and experimental results demonstrate that noise-like waveforms with a "thumbtack"-like ambiguity functions accompanied by properly designed mismatched filters may be used for target detection in heavy clutter in HF-OTHR.

5. REFERENCES

[1] M. I. Skolnik, *Radar Handbook*, McGraw-Hill, 3rd edition, 2008.

[2] R. Price and E. M. Hofstetter, "Bounds on the volume and height distributions of the ambiguity function," *Information Theory, IEEE Transactions on*, vol. 11, no. 2, pp. 207–214, Apr 1965.

[3] G. Fabrizio, *High Frequency Over The Horizon Radar: Fundamental Principles, Signal Processing, and Practical Applications*, McGraw-Hill, 2013.

[4] M. P. Hartnett, J. T. Clancy, and R. J. Denton Jr., "Utilization of a non-recurrent waveform to mitigate range-folded spread doppler clutter. application to over-the-horizon radar," *Radio Science*, vol. 23, no. 4, pp. 1125–1133, July-August 1998.

[5] M. Ravan, R. J. Riddolls, and R. S. Adve, "Ionospheric and auroral clutter models for hf surface wave and over the horizon radar systems," *Radio Science*, vol. 47, pp. RS2010 (1–12), 2012.

[6] D. DeLong and E. M. Hofstetter, "The design of clutter-resistant radar waveforms with limited dynamic range," *Information Theory, IEEE Transactions on*, vol. 15, no. 3, pp. 376–385, May 1969.

[7] L. J. Spafford, "Optimum radar signal processing in clutter," *Information Theory, IEEE Transactions on*, vol. 14, no. 5, pp. 734–743, Sep 1968.

[8] C. Stutt and L. J. Spafford, "A "best" mismatched filter response for radar clutter discrimination," *Information Theory, IEEE Transactions on*, vol. 14, no. 2, pp. 280–287, Mar 1968.

[9] Y. I. Abramovich and M. B. Sverdlik, "Synthesis of generalised ν-filters which ensure zero level of sidelobes within a given zone of the cross-ambiguity function," *Radio Engineering and Electronic Physics*, vol. 15, no. 11, pp. 2085–2087, 1970.